Research Article | Vol. 10, No. 3 / 1 March 2020 / Optical Materials Express 717
Optical Materials EXPRESS

High-resolution absorption measurement at the zero phonon line of Yb:YAG between 80 K and 300 K

MARIASTEFANIA DE VIDO,[1,2,*] AGNIESZKA WOJTUSIAK,[3] AND KLAUS ERTEL[1]

[1] STFC Rutherford Appleton Laboratory, Central Laser Facility, Didcot, OX11 0QX, UK
[2] Institute of Photonics and Quantum Sciences, Heriot-Watt University, Edinburgh, EH14 4AS, UK
[3] Loughborough University, Loughborough, LE11 3TU, UK
[*] mariastefania.de-vido@stfc.ac.uk

Abstract: We present measurements of the temperature dependence of the absorption cross-section of Yb:YAG at the zero phonon line (ZPL) near 969 nm. Experiments were carried out on a 1.08 mm thick, ceramic, 1.1 at-% Yb-doped YAG sample over a temperature range between 80 K and 300 K. Results show that the ZPL characteristics strongly depend on temperature. The absorption cross section increases from $0.8 \cdot 10^{-20}$ cm^2 to above $49 \cdot 10^{-20}$ cm^2 as temperature is decreased from 300 K to 80 K. The full-width at half maximum of the absorption line decreases with temperature, from 2.38 nm at 300 K to 0.05 nm at 80 K. The absorption peak shifts from 969.04 nm at 300 K to 968.39 nm at 80 K. To the best of our knowledge, this is the first time that the ZPL of Yb:YAG has been characterised with enough resolution at cryogenic temperatures and we expect that this data will assist in the design and optimisation of Yb:YAG lasers pumped on this absorption line.

Published by The Optical Society under the terms of the Creative Commons Attribution 4.0 License. Further distribution of this work must maintain attribution to the author(s) and the published article's title, journal citation, and DOI.

1. Introduction

Laser systems capable of generating high energy (from few J to kJ) nanosecond pulses are required for a wide variety of applications. These include materials processing [1], research into extreme states of matter [2] and pumping of petawatt-class femtosecond lasers, which in turn are used for the realisation of compact, high brightness radiation (X-ray and γ-ray) [3] and particle (electron, proton, ion, muon) [4,5] sources for a wide range of applications, including remote high-resolution imaging [6] and medical applications [7,8]. Proof-of-principle demonstrations of most of these applications have so far been carried out using large-scale lasers relying on flash-lamp pumped amplifiers, which are limited in terms of pulse repetition rate and efficiency [9]. However, practicable real-world applications in the industrial and medical sectors require efficient high energy lasers delivering high average powers. Recently, it has been demonstrated that diode-pumped solid state lasers (DPSSLs) are capable of delivering multi-J pulse energy at multi-Hz repetition rate. Yb^{3+}-doped Yttrium Aluminium Garnet (Yb:YAG) has been identified as one of the most suitable active media for high-energy, high repetition rate DPSSLs [10]. Cryogenically-cooled ceramic Yb:YAG is used, for example, for the production of 105 J pulses at 10 Hz (> 1 kW average power) [11] and of 1.5 J pulses at 500 Hz (750 W average power) [12]. The absorption spectrum of Yb:YAG includes two absorption peaks, one around 940 nm and the other, the so-called zero-phonon line (ZPL), around 969 nm [13]. Most Yb:YAG lasers, in particular those operating at low gain medium temperature, have so far been pumped at 940 nm because the broader bandwidth of this line imposes less stringent requirements on pump linewidth and wavelength stability. However, recent improvements in volume Bragg grating

#386436 https://doi.org/10.1364/OME.386436
Journal © 2020 Received 7 Jan 2020; revised 29 Jan 2020; accepted 29 Jan 2020; published 7 Feb 2020

Optical Materials EXPRESS

stabilised diode laser technology enable narrower and more stable pump emission spectra [14], which could pave the way to high power pumping at the ZPL. This would result in lower quantum defect, leading to increased system efficiency and reduced thermal load on the gain medium. As a result, systems would be less affected by unwanted thermal effects, such as aberrations and thermal stress-induced birefringence, and could be operated at higher average powers. The advantages of ZPL pumping have already been confirmed in the case of low-energy Yb:YAG systems, such as thin-disk amplifiers [15]. High-energy, high average power Yb:YAG amplifiers rely on cryogenic cooling to reduce re-absorption losses and to remove waste heat. Information on the temperature dependence of the absorption of Yb:YAG around 940 nm is available in the literature [15,16]. The absorption at the ZPL was included in those measurements, but the spectrographs employed had insufficient resolution to accurately measure the width and the absorption of the line at low temperatures. These measurements showed that the ZPL undergoes thermal narrowing and shift as the temperature is reduced. Previous studies suggest that these mechanisms are due to a combination of homogeneous broadening and electron-phonon coupling effects [17,18]. This paper reports on high resolution characterisation of the ZPL between 80 K and 300 K. We expect that our results will be useful for assessing the feasibility of ZPL pumping for high-energy DPSSLs and for optimising pump sources for Yb:YAG systems.

2. Materials and methods

Initially, absorption measurements were carried out on a 5.13 mm thick, ceramic, 1.1 atom-% Yb^{3+}-doped YAG sample. However, results showed that absorption by this sample was too strong at low temperatures to correctly characterise the ZPL. As a result, a second round of measurements, reported in this paper, was carried out on a thinner 1.1 atom-% Yb^{3+}-doped ceramic YAG sample with a size of 24.3 mm x 24.3 mm x 1.08 mm, manufactured by Konoshima Chemical (Japan) and polished on both square surfaces by Baikowski International (Japan). The square surfaces are plane parallel and are anti-reflection (AR) coated to achieve <0.2% reflection per surface between 920 nm and 1050 nm for angles of incidence between 0° and 10°. Figure 1 shows the experimental setup used to characterise the ZPL.

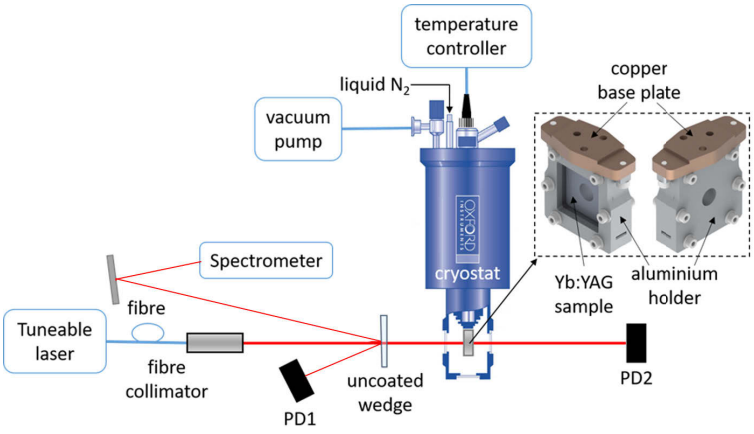

Fig. 1. Experimental setup used to characterise absorption at the ZPL of Yb:YAG (PD1, PD2 = photo-detectors). The insert shows frontal and rear views of the holder in which the Yb:YAG sample is mounted.

The radiation source used for the measurement is a continuous wave fibre-coupled external cavity diode laser (LION P-960-0117-00998, Sacher Laser), tunable over the spectral range between 920 nm and 985 nm and with a linewidth of <20 kHz. The output beam, with a power of

Optical Materials EXPRESS

around 15 mW, is collimated by a fibre collimator and directed onto the Yb:YAG sample under study, which is located inside an optical cryostat (Optistat DN-V2, Oxford Instruments). The sample, oriented normal to the incident beam, is mounted directly under the heat exchanger of the cryostat using a copper base plate and an aluminium holder. The holder provides contact onto the whole back surface of the sample with the exception of a 8 mm diameter aperture to allow transmission of the laser beam (see insert in Fig. 1). Indium foil is placed between sample and holder surfaces to improve thermal contact. The temperature is measured using a platinum resistance thermometer attached to the copper plate. Fused silica wedged windows, AR coated to reduce surface reflectivity below 0.5%, allow optical access to the sample. Two silicon photo-detectors (PH100-Si-HA, Gentec-EO) monitor the power incident onto and transmitted through the sample. The first, indicated in Fig. 1 as PD1, measures the power of the beam reflected off the front surface surface of an uncoated fused silica wedge. The second one, indicated as PD2, measures the power transmitted through the sample. Before the experiment, the power incident onto the Yb:YAG sample was calibrated by positioning PD2 directly behind the wedge and by simultaneously measuring signals provided by PD1 and PD2. Optical losses introduced by the cryostat windows were determined as a function of the wavelength by measuring transmission through the system without the Yb:YAG sample in the beam path. Background signals on PD1 and PD2 were measured and subtracted for all power measurements. A high resolution spectrometer (Laser Spectrum Analyser, HighFinesse GmbH), coupled with a single mode fibre, measures the wavelength of the light reflected off the back surface of the wedge. The absolute accuracy of the spectrometer is 5 pm and the sensitivity for change in wavelength is 1 pm. The spectrometer was calibrated with a helium-neon laser.

3. Measurement results

The absorption cross-section of Yb:YAG at the ZPL was calculated using Lambert-Beer's law [19]:

$$\sigma_a(\lambda) = \ln\left(\frac{I_i(\lambda)}{I_t(\lambda)}\right)/N_{dop}L, \tag{1}$$

where λ is the wavelength of light, $I_i(\lambda)$ and $I_t(\lambda)$ are the power incident onto and transmitted through the sample, respectively, N_{dop} is the density of dopant Yb^{3+} ions and L is the thickness of the sample. For 1.1 atom-% Yb^{3+}-doped YAG, $N_{dop} = 1.52 \cdot 10^{20}$ cm^{-3}. Absorption measurements were carried out for a number of discrete temperatures between 80 K and 300 K. The wavelength was changed in nominal steps of 0.01 nm for measurements between 300 K and 150 K; 0.0025 nm at 125 K and 100 K; and 0.001 nm at 80 K. Data shown in this article is available at [20]. Figure 2 shows the transmission through the sample as a function of wavelength at 80 K, 100K, 200 K and 300 K. The transmission at the ZPL centre is 1.12%, 68.8% and 87.6% at 100 K, 200 K and 300 K, respectively. When the temperature is reduced to 80 K, transmission at maximum absorption approaches 0%.

Figures 3(a) and 3(b) show, in more detail, transmission measurements as a function of the wavelength at 80 K and 100 K, respectively. Figure 3(c) shows data points collected at 80 K over a small wavelength range around the ZPL absorption peak. It is possible to notice that the measured transmission remains fairly constant over a small range around the line centre. This indicates that, over this range, the incident beam is completely absorbed because the sample is still too thick. A lower-absorption sample is therefore required for accurate characterisation of the ZPL at 80 K. The 0.03% transmission signal at maximum absorption provides an upper limit to the estimate of the spectral impurity of the source. This data, once processed using Eq. (1), provides a lower limit to the actual absorption cross-section at 80 K. However, given the small spectral range over which the sample absorbs all of the incoming light, the data still provides a good estimate of the width of the absorption line and of the peak wavelength at 80 K. Figure 3(d) shows a similar view of data collected at 100 K. In this case, the lack of flattening of the curve at

Optical Materials EXPRESS

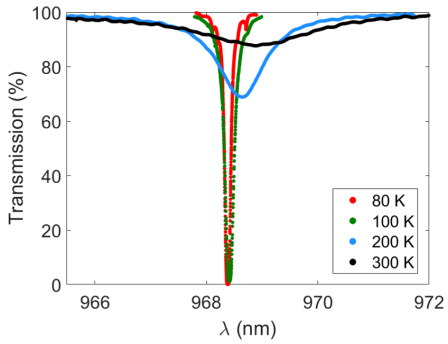

Fig. 2. Transmission through the sample at the ZPL at 80 K, 100 K, 200 K and 300 K.

the centre of the line and the higher value of transmission indicate that the measured transmission is largely unaffected by systematic errors such as spectral impurity.

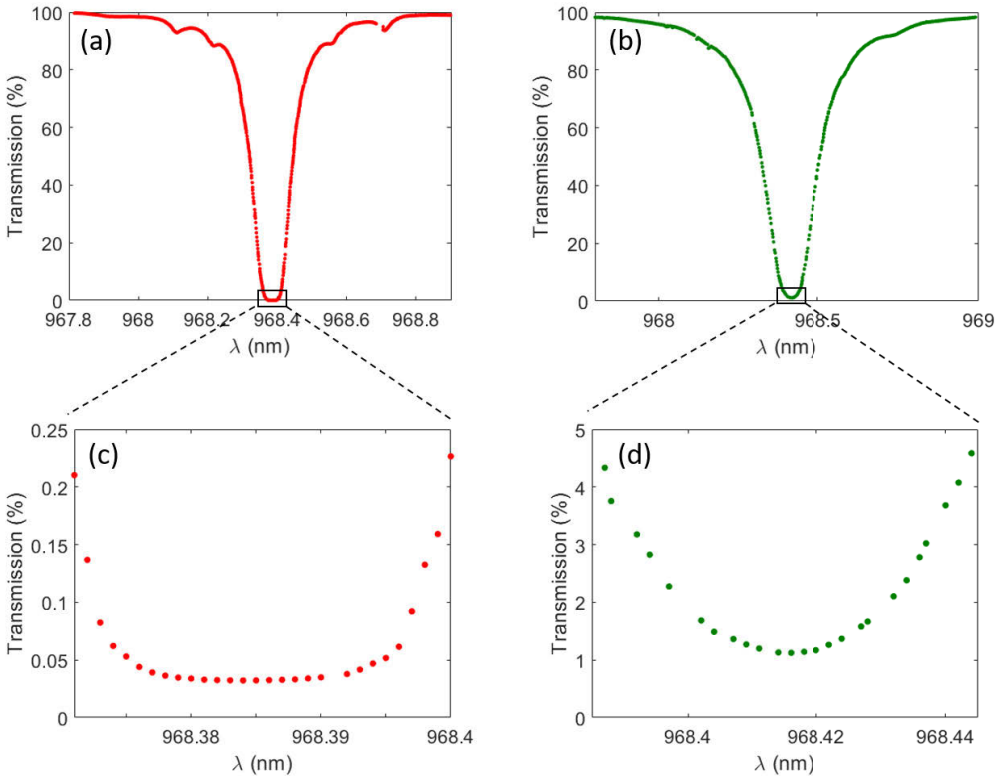

Fig. 3. Transmission through the sample as a function of wavelength at 80 K (a) and at 100 K (b). Zoomed-in views of the measurement at the centre of the ZPL at 80 K (c) and at 100 K (d).

Figure 4(a) shows the absorption cross-section, calculated using Eq. (1), at the ZPL at temperatures between 80 K and 150 K and Fig. 4(b) between 175 K and 300 K. Some spectra show oscillations consistent with an etalon effect caused by the sample. Oscillations are more apparent at higher temperature because etalon finesse increases with decreasing absorption.

Optical Materials EXPRESS

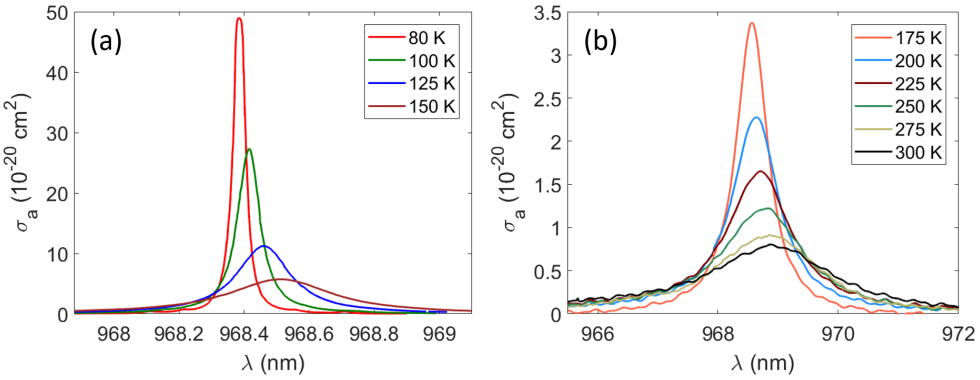

Fig. 4. Absorption cross-section at the ZPL of Yb:YAG at temperatures between 80 K and 150 K (a) and between 175 K and 300 K (b).

Figure 5 summarises the temperature dependence of the full-width at half maximum (FWHM) linewidth (a), of the peak wavelength (b) and of the peak absorption cross-section (c).

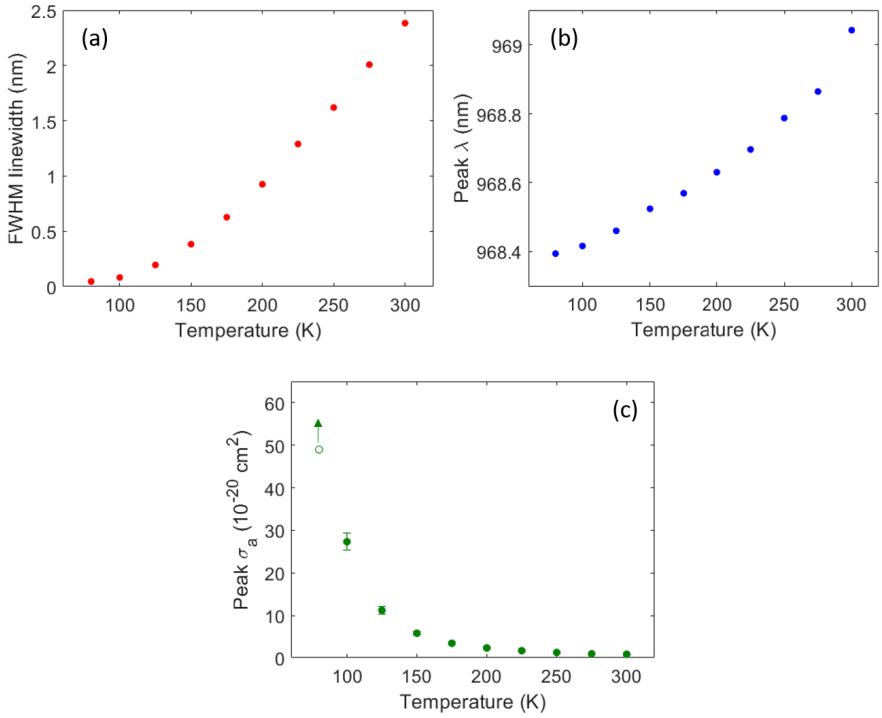

Fig. 5. ZPL characteristics between 80 K and 300 K: FWHM linewidth (a), peak wavelength (b) and peak absorption cross-section (c). The data point at 80 K represents a lower limit to the actual value of the absorption cross-section.

At 300 K, the ZPL is centred at 969.04 nm, with a peak absorption cross-section of $0.8 \cdot 10^{-20}$ cm^2 and a FWHM linewidth of 2.38 nm, in agreement with data published in [21,22]. As the temperature is decreased, the FWHM linewidth reduces, reaching 0.05 nm at 80 K (Fig. 5(a)), and the peak wavelength shifts to lower values, with 968.39 nm measured at 80 K (Fig. 5(b)). At the same time, the peak absorption cross-section sharply increases (Fig. 5(c)), reaching $28 \cdot 10^{-20}$

Optical Materials EXPRESS

cm^2 at 100 K and a value above $49 \cdot 10^{-20}$ cm^2 at 80 K. Error bars in Fig. 5(c) take into account uncertainty in the laser power measurement (±5%), in sample doping concentration (±1.8% relative) and in the amount of sample material thickness (±0.9%).

The narrow linewidth of the ZPL at low temperatures constitutes the main challenge towards ZPL pumping because it imposes tight demands on pump linewidth and wavelength stability. The feasibility of ZPL pumping at low temperatures needs to be investigated along with the practical implications of the high absorption cross-section and of the resulting low saturation fluence. We have started work on modelling pump absorption to analyse the feasibility of ZPL pumping for high-energy, high average power DPSSLs.

4. Conclusion

In this paper, we investigated the temperature dependence of the absorption cross-section near the ZPL of Yb:YAG between 80 K and 300 K. To the best of our knowledge, this is the first time that the ZPL of Yb:YAG has been characterised with sufficient resolution at low temperatures. Measurements show that peak absorption cross-section and FWHM linewidth strongly depend on the temperature of the material. The FWHM linewidth reduces from 2.38 nm at 300 K to 0.05 nm at 80 K, while the peak absorption cross section increases from $0.8 \cdot 10^{-20}$ cm^2 to above $49 \cdot 10^{-20}$ cm^2. The absorption peak shifts from 969.04 nm at 300 K to 968.39 nm at 80 K. We expect that these results will be useful for the design and optimisation of Yb:YAG lasers pumped at the ZPL.

Funding

Royal Commission for the Exhibition of 1851 (Industrial Fellowship); Laserlab-Europe (654148); Engineering and Physical Sciences Research Council (1979259).

Disclosures

The authors declare that there are no conflicts of interest related to this article.

References

1. A. Azhari, S. Sulaiman, and A. K. Prasada Rao, "A review on the application of peening processes for surface treatment," IOP Conf. Ser.: Mater. Sci. Eng. **114**, 012002 (2016).
2. M. McMahon and U. Zastrau, *et al*, "Conceptual Design Report: Dynamic Laser Compression Experiments at the HED Instrument of European XFEL XFEL," EU TR-2017-001 (2017).
3. S. Kneip, S. R. Nagel, C. Bellei, N. Bourgeois, A. E. Dangor, A. Gopal, R. Heathcote, S. P. D. Mangles, J. R. Marqus, A. Maksimchuk, P. M. Nilson, K. T. Phuoc, S. Reed, M. Tzoufras, F. S. Tsung, L. Willingale, W. B. Mori, A. Rousse, K. Krushelnick, and Z. Najmudin, "Observation of synchrotron radiation from electrons accelerated in a petawatt-laser-generated plasma cavity," Phys. Rev. Lett. **100**(10), 105006 (2008).
4. S. P. D. Mangles, C. D. Murphy, Z. Najmudin, A. G. R. Thomas, J. L. Collier, A. E. Dangor, E. J. Divall, P. S. Foster, J. G. Gallacher, C. J. Hooker, D. A. Jaroszynski, A. J. Langley, W. B. Mori, P. A. Norreys, F. S. Tsung, R. Viskup, B. R. Walton, and K. Krushelnick, "Monoenergetic beams of relativistic electrons from intense laser-plasma interactions," Nature **431**(7008), 535–538 (2004).
5. H. Schwoerer, S. Pfotenhauer, O. Jckel, K. U. Amthor, B. Liesfeld, W. Ziegler, R. Sauerbrey, K. W. D. Ledingham, and T. Esirkepov, "Laser-plasma acceleration of quasi-monoenergetic protons from microstructured targets," Nature **439**(7075), 445–448 (2006).
6. C. M. Brenner, S. R. Mirfayzi, D. R. Rusby, C. Armstrong, A. Alejo, L. A. Wilson, R. Clarke, H. Ahmed, N. M. H. Butler, D. Haddock, A. Higginson, A. McClymont, C. Murphy, M. Notley, P. Oliver, R. Allott, C. Hernandez-Gomez, S. Kar, P. McKenna, and D. Neely, "Laser-driven X-ray and neutron source development for industrial applications of plasma accelerators," Plasma Phys. Controlled Fusion **58**(1), 014039 (2016).
7. U. Masood, M. Bussmann, T. E. Cowan, W. Enghardt, L. Karsch, F. Kroll, U. Schramm, and J. Pawelke, "A compact solution for ion beam therapy with laser accelerated protons," Appl. Phys. B **117**(1), 41–52 (2014).
8. J. M. Cole, J. C. Wood, N. C. Lopes, K. Poder, R. L. Abel, S. Alatabi, J. S. J. Bryant, A. Jin, S. Kneip, K. Mecseki, D. R. Symes, S. P. D. Mangles, and Z. Najmudin, "Laser wakefield accelerators as hard x-ray sources for 3D medical imaging of human bone," Sci. Rep. **5**(1), 13244 (2015).
9. G. Miller, E. Moses, and C. Wuest, "The national ignition facility," Opt. Eng. **43**(12), 2841–2853 (2004).

Optical Materials EXPRESS

10. W. F. Krupke, "Ytterbium solid-state lasers. The first decade," IEEE J. Sel. Top. Quantum Electron. **6**(6), 1287–1296 (2000).
11. P. Mason, M. Divoky, K. Ertel, J. Pilar, T. Butcher, M. Hanus, S. Banerjee, J. Phillips, J. Smith, M. De Vido, A. Lucianetti, C. Hernandez-Gomez, C. Edwards, T. Mocek, and J. Collier, "Kilowatt average power 100 J-level diode pumped solid state laser," Optica **4**(4), 438–439 (2017).
12. C. Baumgarten, M. Pedicone, H. Bravo, H. Wang, L. Yin, C. S. Menoni, J. J. Rocca, and B. A. Reagan, "1 J, 0.5 kHz repetition rate picosecond laser," Opt. Lett. **41**(14), 3339–3342 (2016).
13. L. D. DeLoach, S. A. Payne, L. L. Chase, L. K. Smith, W. L. Kway, and W. F. Krupke, "Evaluation of absorption and emission properties of Yb-doped crystals for laser applications," IEEE J. Quantum Electron. **29**(4), 1179–1191 (1993).
14. B. L. Volodin, S. V. Dolgy, E. D. Melnik, E. Downs, J. Shaw, and V. S. Ban, "Wavelength stabilization and spectrum narrowing of high-power multimode laser diodes and arrays by use of volume Bragg gratings," Opt. Lett. **29**(16), 1891–1893 (2004).
15. D. C. Brown, R. L. Cone, Y. Sun, and R. W. Equall, "Yb:YAG absorption at ambient and cryogenic temperatures," IEEE J. Sel. Top. Quantum Electron. **11**(3), 604–612 (2005).
16. J. Körner, V. V. Jambunathan, J. Hein, R. Seifert, M. Loeser, M. Siebold, U. Schramm, P. Sikocinski, A. Lucianetti, T. Mocek, and M. C. Kaluza, "Spectroscopic characterization of Yb^{3+}-doped laser materials at cryogenic temperatures," Appl. Phys. B **116**(1), 75–81 (2014).
17. G. A. Borgomolova, D. N. Vylegzhanin, and A. A. Kaminskiĭ, "Spectral and lasing investigations of garnets with Yb^{3+} ions," Sov. Phys.-JEPT **42**(3), 440–446 (1976).
18. D. Hsu and J. L. Skinner, "On the thermal broadening of zero-phonon impurity lines in absorption and fluoresence spectra," J. Chem. Phys. **81**(4), 1604–1613 (1984).
19. W. Koechner, *Solid-State Laser Engineering* (Springer, 2010).
20. eData: STFC Research Data Repository, http://dx.doi.org/10.5286/edata/737.
21. K. Beil, S. T. Fredrich-Thornton, F. Tellkamp, R. Peters, C. Kränkel, K. Petermann, and G. Huber, "Thermal and laser properties of Yb:LuAG for kW thin disk lasers," Opt. Express **18**(20), 20712 (2010).
22. J. Koerner, C. Vorholt, H. Liebetrau, M. Kahle, D. Kloepfel, R. Seifert, J. Hein, and M. Kaluza, "Measurement of temperature-dependent absorption and emission spectra of Yb:YAG, Yb:LuAG, and Yb:CaF_2 between 20 °C and 200 °C and predictions on their influence on laser performance," J. Opt. Soc. Am. B **29**(9), 2493–2502 (2012).

192.41.114.227 {ts '2020-04-07 05:45:25'}